31.0 ACCUMULATIVE ROLL BONDING OF AL AND TI SHEETS TOWARD LOW TEMPERATURE SUPERPLASTICITY

Brady McBride (Mines)
Faculty: Kester Clarke (Mines)
Industrial Mentor: Ravi Verma (Boeing) and John Carpenter (LANL)

This project initiated in Fall 2017 and is supported by K. Clarke's startup. The research performed during this project will serve as the basis for a Ph.D. thesis program for Brady McBride.

31.1 Project Overview and Industrial Relevance

Accumulative roll bonding (ARB) is a severe plastic deformation technique used to produce ultra-fine grain material by introducing large plastic strains within a material [31.1]. The surfaces of two sheets are commonly wire-brushed before being stacked and roll bonded together in a conventional rolling mill [31.1]. After rolling, the material is sectioned in half and the process is repeated. A single-pass, 50% rolling reduction is commonly employed to ensure adequate bonding and to retain the sample's original dimensions after each roll bonding cycle [31.1]. The ARB process is largely different from conventional rolling processes in that heavy single-pass reductions are conducted without lubrication. This imparts redundant shear into the surface of the rolled material, which is introduced through the material's thickness with subsequent roll bonding cycles [31.2], ultimately leading to grain refinement.

The attraction to ARB lies in the ability to produce ultra-fine-grained material with conventional processing equipment while maintain consistent sample geometry. With the accumulation of large strains, dislocation cell structures form within the material that further develop into refined grains [31.3-4]. Ultra-fine grains (~250 nm) produced after 5 cycles of ARB in Al 5083 have exhibited tensile elongations in excess of 200% for strain rates of 10^{-3} s^{-1} at 200 °C [31.5]. In comparison, superplastic Al 5083 produced with conventional processing methods typically requires temperatures of 500 °C and strain rates of no greater than 10^{-3} s^{-1} to produce elongations of around 300 %. Enhanced superplasticity provided by the ARB process would be beneficial to superplastic sheet forming operations, where reduced temperatures and/or increased strain rates could lead to cost savings and reduced die wear.

31.2 Previous Work – 5 Successful Cycles of Al 5083 with Reduced Edge Cracking

One of the limitations of ARB is the development of edge cracking, which generally occurs as a result of material overhang, lateral spreading or a combination of both. Material overhang cracking occurs due to poor sheet alignment as the material enters the mill; this can be mitigated by wire binding the sheets to restrict movement during rolling. Edge cracking due to lateral spreading is commonly reported in literature [31.1,31.4], but mitigation strategies have not been presented in much detail.

Lateral spreading occurs during rolling at the edges of severely deformed sheet due to the lack of lateral constraint. While edge cracking can be reduced with increased sheet width, this necessitates increased rolling loads. Artificially imposing lateral constraint is thought to reduce spreading for narrow sheets, and therefore reduce edge cracking. Such a constraint was applied to roll-bonded Al 5083 samples by rolling within a sacrificial "window" of Al 1100 that has the same starting thickness of two 5083 sheets. Upon rolling, the Al 1100 laterally spreads and constrains the Al 5083 sheets, thus reducing the lateral spreading of the sheets by about 50 %. This technique was applied to 5 successful cycles of Al 5083 to produce samples with minimal edge cracking; **Figure 31.1** shows a comparison of samples with and without imposed lateral constraint.

31.3 Recent Progress

31.3.1 Microstructural Characterization of 5 Cycle ARBed Al 5083

Microstructural characterization of the 5-cycle ARBed Al 5083 was conducted using both transmission electron microscopy (TEM) and electron backscatter diffraction (EBSD). Previous attempts at EBSD with an Ar ion-milled

surface showed suboptimal results due to the presence of surface artefacts on the length scale of microstructural features, making it difficult to obtain clear Kikuchi patterns during EBSD analysis. The surface preparation procedure has since been changed to bulk electropolishing, where a surface sufficient for EBSD can be obtained without inducing mechanical polishing damage.

Misorientation plots from EBSD scans of the 5-cycle ARBed Al 5083 as shown in **Figure 31.2** have been used to quantify grain size and grain boundary development. The grains appear to be mostly equiaxed with a mean grain size around 1 μm in the RD-TD plane, but seem to be elongated parallel to the rolling direction in the RD-ND plane with a mean grain size of about 250 nm by 1 μm. The grains in the RD-ND plane appear to consist of mainly high angle grain boundaries (HAGBs), with 80 % of boundaries having misorientation greater than 15°. The grains in the RD-TD plane are mostly comprised of HAGBs (68%). HAGBs are preferential for grain boundary sliding, which is a primary deformation mechanism in conventional high temperature superplasticity. From these observations of the microstructure, it is apparent that the ARBed material has a three-dimensional grain morphology that should be consistently examined before and after superplastic deformation to better understand the pertinent deformation mechanisms.

31.3.2 High Temperature Tensile Testing

High temperature tensile testing for superplasticity was conducted on the Al 5083 5 ARB samples as well as samples that had been conventionally rolled and recrystallized to achieve a uniform 15 μm grain structure. The latter material serves as a baseline to represent commercial superplastic 5083 aluminum, which typically has a grain size on the order of 10 – 15 μm. Tensile tests were conducted using a natural convection clamshell furnace on an Instron load frame. A prototype grip fixture designed to reduce error during superplasticity testing was machined at CSM out of 303 stainless steel and was used for these tests. A thermal gradient between the grip and gauge section ranging between 5 – 7 °C (about 1.5 % of the target absolute temperature) was achieved prior to the start of deformation with a 5-minute soak time. Tensile tests were conducted using a constant crosshead speed at an initial strain rate of 10^{-3} s^{-1}. Due to the small tensile loads, the compliance of the frame was assumed to be negligible compared to the tensile elongations, and so crosshead displacement was taken as a direct measure of strain.

The as-deformed tensile specimens are shown in **Figure 31.3** where it is evident the 5-cycle ARBed Al 5083 specimens showed consistently higher elongations that the conventionally recrystallized material. Diffuse and localized necks are present in all samples apart from the ARBed sample tested at 377 °C (hereafter referred to as A377). Extreme tensile elongations in superplasticity are attributed to a high strain rate sensitivity which inhibits the localization of strain. In fact, superplasticity is commonly defined as having a high strain rate sensitivity, typically with an *m* value greater than 0.3 as measured by strain rate jump tests. By examining the neck formation across samples in **Figure 31.3**, it appears that only sample A377 demonstrated a true superplastic response by inhibiting localized necking. Additional tensile testing is needed to determine whether superplasticity has been achieved at lower temperatures on the basis of having a sufficient *m* value. Regardless of the nature of deformation, it is evident that enhanced *ductility* was achieved by the ARB process over the conventionally recrystallized material.

The data from these tensile tests in shown in **Figure 31.4** with comparison to work done by Tsuji et al. in a very similar study [31.5]. Although the general flow curves are comparable at each testing temperature, it is clear there is a divergence in behavior with increased temperature; this may indicate that subtle differences in processing and mechanical testing methodologies may lead to significantly different tensile results. A more detailed comparison between the results herein and the works of Tsuji et al. is needed to reach more substantial conclusions.

31.3.3 Roll Bonding Trials at Los Alamos National Laboratory (LANL)

Roll bonding trials of wider sheets of Al 5083 were conducted at Los Alamos National Laboratory (LANL). Los Alamos has a large scale, two-high rolling mill with 18” diameter rolls. Rolling on a larger mill has the potential to provide two key benefits. Firstly, a higher capacity mill allows for wider samples to be roll bonded, which will have less of a stress gradient due to lateral spreading and will therefore be less prone to edge cracking. Secondly, a mill with larger rolls is thought to impart more redundant shear into the material, which may lead to more significant grain refinement. Neither of these topics have been well documented in literature.

The initial trials of Al 5083 highlighted the fact that successful roll bonding of aluminum, being relatively soft, is very sensitive to the roll alignment; a few thousandths of an inch of mis-alignment along the length of the roll gap causes one side of the sample to elongate more than the other side, resulting in curling and buckling. A strategic plan to calibrate the rolls for roll bonding aluminum is planned for the next trial at LANL, which will allow for trials of wider and harder samples, such as titanium alloys.

31.3.4 Preliminary Cavitation Study

Superplasticity is characterized by a high strain rate sensitivity (m>0.3) such that the tendency to form a localized neck is suppressed. As a result, superplastic samples generally fail by cavity coalescence, whereby small cavities nucleate at discontinuities in the matrix and continue to grow as the sample is strained. Cavitation is thought to be caused by strain discontinuities at grain boundaries and precipitates, which nucleate during grain boundary sliding. Preliminary investigation of the as-tensile-tested cross-sections only show cavity formation in the A377 specimen, suggesting this is the only sample that underwent extensive grain boundary sliding.

Image analysis was conducted on the cross-section of the A377 tensile specimen to quantify cavity formation, as shown in **Figure 31.4.** From the void intensity plot in **Figure 31.4b**, it is apparent that voids preferentially nucleate at periodic locations across the sample thickness, which correlates to the different bonding layers. Two important observations are deduced from this plot. Firstly, it is noted that large void intensities are present at locations midway, quarter way, and semi-quarter way through the sample, corresponding to the most recent, 2nd most recent and 3rd most recent bond interface. It is interesting to see that the most recent bond at the centerline does not have the highest void percentage; this perhaps indicates the "weakest" bond is not necessarily detrimental to superplastic performance. Secondly, the smallest distinguishable interval between void intensity peaks is roughly 15 μm, which corresponds the thickness of each individual layer of material after 5 cycles of ARB. This confirms that voids preferentially nucleate at layer interfaces and illustrates the fact that interfacial layers can perhaps be used to control the size and location of voids. As superplastic deformation typically terminates with excessive cavitation coalescence, it will be useful to understand the nucleation and growth of cavities during high temperature deformation.

31.4 Plans for Next Reporting Period

Preliminary high temperature tensile tests have demonstrated enhanced superplasticity in 5 ARBed Al 5083. Additional steps will be taken to in the upcoming months to further this project, including:

- High temperature tensile testing on 5 ARBed Al 5083 to measure strain rate sensitivity (m-value).
- Microstructural characterization on samples previously tested for superplasticity.
- TEM characterization of bond interfaces obtained with focused ion beam (FIB) lift-out.
- Continued literature review on the compositional effects of dispersoid strengthening and enhanced grain refinement of Al 5XXX alloys.

31.5 References

[31.1] Y. Saito, H. Utsunomiya, N. Tsuji, T. Sakai, Novel Ultra-High Straining Process For Bulk Materials - Development of the Accumulative Roll Bonding (ARB) Process, Acta Materialia. 47 (1999) 579–583.

[31.2] S.H. Lee, Y. Saito, N. Tsuji, H. Utsunomiya, T. Sakai, Role of shear strain in ultragrain refinement by accumulative roll-bonding (ARB) process, Scripta Materialia. 46 (2002) 281–285.

[31.3] Y. Saito, N. Tsuji, H. Utsunomiya, T. Sakai, R. Hong, Ultra-fine grained bulk aluminum produced by accumulative roll-bonding (ARB) process, Scripta Materialia. 40 (1999) 795–800.

[31.4] M. Reza, F. Ashrafizadeh, R. Jamaati, On the use of accumulative roll bonding process to develop nanostructured aluminum alloy 5083, Materials Science & Engineering A. 561 (2013) 145–151.

[31.5] N. Tsuji, K. Shiotsuki, Y. Saito, Superplasticity of Ultra-Fine Grained Al-Mg Alloy by Accumulative Roll Bonding, Mater. Trans. 40 (1999) 765–771.

31.6 Figures and Tables

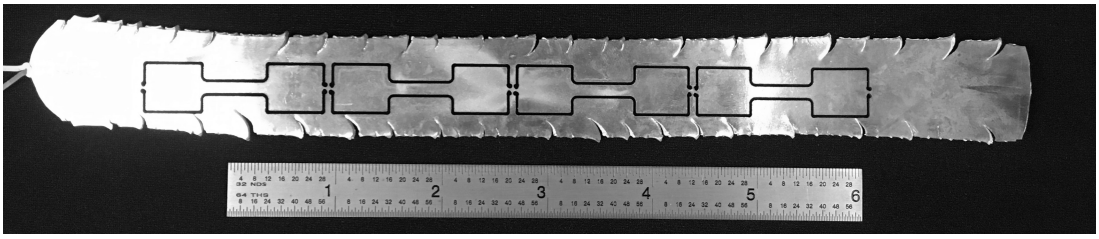

(a)

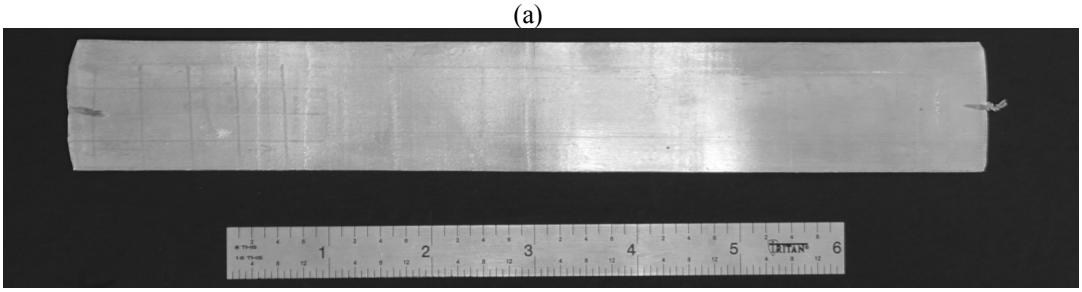

(b)

Figure 31.1: Edge quality of 5-cycle ARBed Al 5083. Subfigure (a) shows a sample roll-bonded without lateral constraint while (b) shows a sample that was rolled within an Al 1100 "window" to artificially impose lateral constraint. The sample in (a) originally started at 2" wide, but had to be sheared after each cycle to remove edge cracks, while the sample in (b) remained at a constant width of 1.25" throughout each bonding cycle.

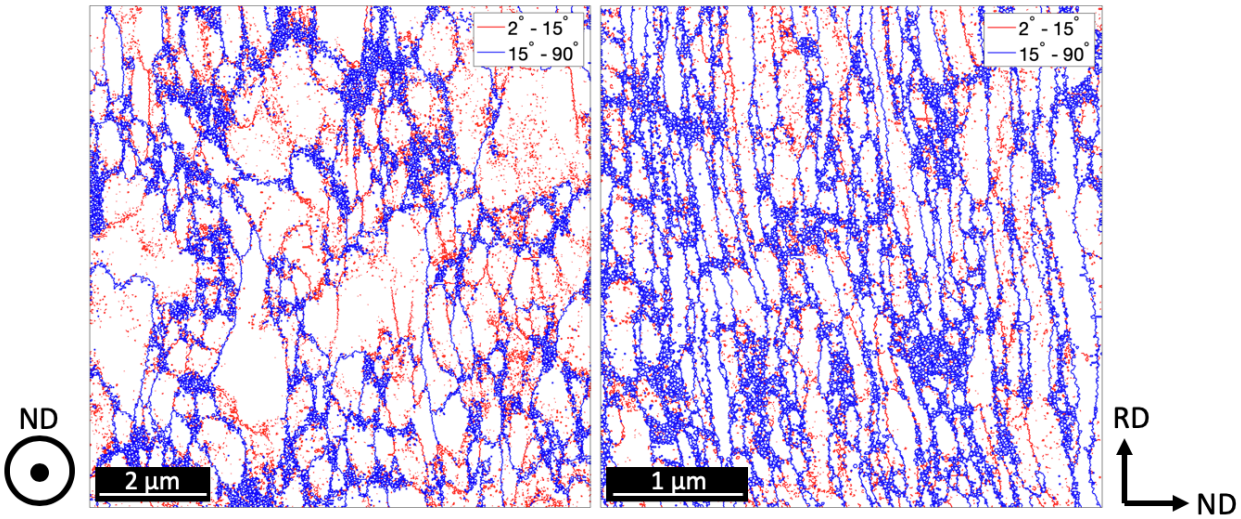

(a) (b)

Figure 31.2: Grain boundary misorientation maps obtained from EBSD of 5-cycle ARBed Al 5083. Subfigure (a) shows the rolling plane containing the RD and TD, while subfigure (b) shows the transverse plane containing the RD and ND. The percentages of HAGB was calculated to be 68% and 80% for subfigures (a) and (b), respectively.

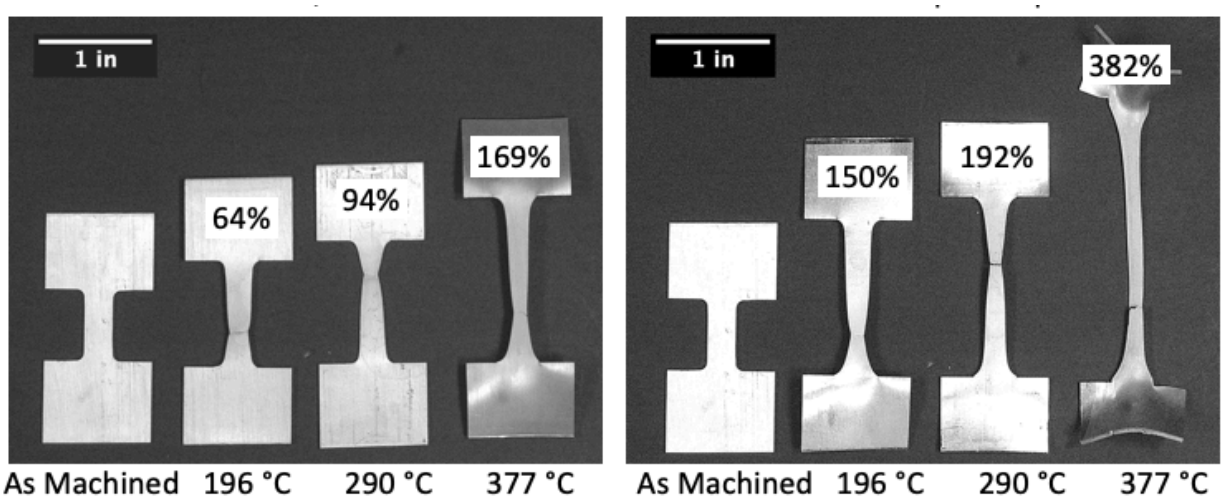

(a) (b)

Figure 31.3: Tensile specimens after elevated temperature testing for superplasticity with initial strain rate of 10^{-3} s^{-1}, operating with constant crosshead displacement. Subfigure (a) shows conventionally recrystallized Al 5083 with ~15 µm grain size while subfigure (b) shows 5-cycle ARBed Al 5083 with ~250 nm x 1 µm x 1 µm grain size. Note a prototype superplastic grip design was used for these tests, which lead to noticeable distortion of the 377 °C samples in the grip regions.

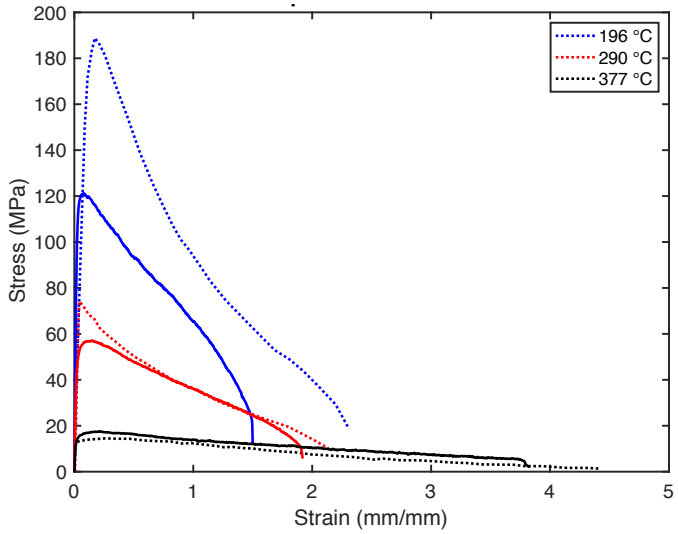

Figure 31.3: Engineering stress-strain curves for 5 ARBed Al 5083 tensile tested with initial strain rate of 10^{-3} s^{-1}, operating with constant crosshead displacement. The solid lines represent data from samples produced within the context of this report, while the dashed lines represent data from a similar study (same processing route, deformation temperature and strain rate) by Tsuji et al. [31.5].

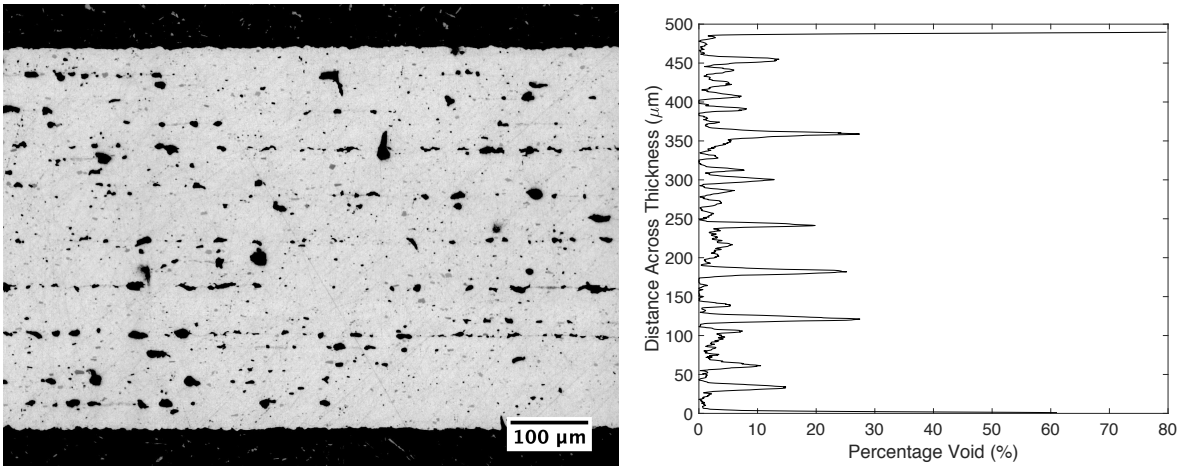

(a) (b)

Figure 31.4: (a) Light optical microscopy (LOM) image of the transverse cross-section of 5 ARB specimen (A377) strained to 382 % at 377 °C and an initial strain rate of 10^{-3} s^{-1}. Subfigure (b) shows intensity distribution of voids across the thickness of the specimen. Note that void location is strongly correlated to layer interface location.